



# The predictive value of energy spectral CT parameters for assessing Ki-67 expression of lung cancer

Peipei Dou<sup>1,2#</sup>, Zhongxiao Liu<sup>1#</sup>, Lixiang Xie<sup>1</sup>, Chong Meng<sup>1</sup>, Chen Wang<sup>1</sup>, Yingying Cui<sup>3</sup>, Chunfeng Hu<sup>1,2</sup>, Guangjun Cheng<sup>1</sup>, Jyhcheng Chen<sup>2,4</sup>, Yankai Meng<sup>1,2\*</sup>, Kai Xu<sup>1,2\*</sup>

<sup>1</sup>Department of Radiology, Affiliated Hospital of Xuzhou Medical University, Xuzhou, China; <sup>2</sup>College of Medical Imaging, Xuzhou Medical University, Xuzhou, China; <sup>3</sup>Department of Pathology, Affiliated Hospital of Xuzhou Medical University, Xuzhou, China; <sup>4</sup>Department of Biomedical and Radiological Sciences, National Yang-Ming University, Taipei

*Contributions:* (I) Conception and design: K Xu, Y Meng; (II) Administrative support: K Xu, G Cheng, C Hu, J Chen; (III) Provision of study materials or patients: Z Liu, C Meng, C Wang, Y Cui; (IV) Collection and assembly of data: P Dou, Z Liu, L Xie; (V) Data analysis and interpretation: P Dou, Y Meng; (VI) Manuscript writing: All authors; (VII) Final approval of manuscript: All authors.

<sup>#</sup>These authors are co-first authors to this work.

<sup>\*</sup>These authors contributed equally to this work.

*Correspondence to:* Kai Xu, MD; Yankai Meng, MD. Department of Radiology, Affiliated Hospital of Xuzhou Medical University, 99 Huaihai West Road, Quanshan District, Xuzhou 221000, China; College of Medical Imaging, Xuzhou Medical University, 209 Tongshan Road, Yunlong District, Xuzhou 221000, China. Email: mengyankai@126.com; xkpaper@163.com.

**Background:** To investigate the predictive value of energy spectral CT parameters for Ki-67 expression in lung cancer.

**Methods:** In this retrospective analysis, 27 primary lung cancer patients confirmed by pathological examination were enrolled between December 2018 and February 2019. All patients underwent baseline arterial phase (AP) and venous phase (VP) energy spectral CT scanning followed by surgery in our institution. The iodine concentration (IC), normalized iodine concentration (NIC) and the slope of 40-80 keV energy spectrum curve ( $\lambda_{HU}$ ) were derived from dual-energy virtual imaging on a Siemens postprocessed workstation. Immunohistochemical examination was performed to analyze Ki-67 expression. The ROC curves were used for predicting the performance of energy spectral parameters for Ki-67 expression.

**Results:** The tumors appeared larger in Ki-67 high expression group than the low expression group ( $P=0.046$ ). The energy spectral parameters were higher in venous phase when compared to arterial phase, but only the venous phase NIC (vpNIC) was significantly different from that of the arterial phase NIC (apNIC) ( $P<0.01$ ). There are significant differences in high and low Ki-67 expression groups for vpNIC and venous  $\lambda_{HU}$  (vp $\lambda_{HU}$ ), ( $P=0.033$  and  $0.037$  for vpNIC and vp $\lambda_{HU}$ , respectively). vpNIC ROC analysis showed borderline P value ( $P=0.056$ ) with an AUC, sensitivity (SE), specificity (SP) and cut-off value (0.717, 92.86, 61.54 and  $\leq 0.347$ ), respectively. The AUC, SE, SP and cut-off value of vp $\lambda_{HU}$  were 0.698, 92.86, 53.85 and  $\leq 2.407$ , respectively.

**Conclusions:** The energy spectral parameters (NIC and  $\lambda_{HU}$ ) of venous phase might be used for predicting Ki-67 stratification. The venous phase energy spectral parameters were higher than the arterial phase. Furthermore, low expression Ki-67 group showed association with higher IC, NIC and  $\lambda_{HU}$  than high expression group.

**Keywords:** Lung cancer; Ki-67 expression; energy spectral parameters; computed tomography

Submitted Dec 11, 2019. Accepted for publication Jun 03, 2020.

doi: 10.21037/tcr-19-2769a

View this article at: <http://dx.doi.org/10.21037/tcr-19-2769a>

## Introduction

In 2017, the number of new lung cancer cases was estimated to be 222,500 in the United States. Lung cancer is the first leading cause of cancer-related deaths in both males as well as females (1). In reality, the vast majority of patients were detected in advanced stages, losing the opportunity of surgery. Even after undergoing individualized treatment such as neoadjuvant therapy, targeted therapy and immunotherapy, the 5-year survival rate of lung cancer in patients remained relatively low at present (2).

Tumor proliferation and differentiation are significantly associated with treatment response and outcomes. Ki-67 is a nuclear protein that is associated with cell proliferation (3). It acts as one of the immunohistochemical (IHC) biomarkers in lung cancer, and is significantly related to the treatment response and outcomes (4). High expression of Ki-67 is correlated with relatively poorer treatment response and worse long-time prognosis in lung cancer (5). IHC examination of biopsy/surgical excision specimens are mainly used for evaluating relevant Ki-67 antigen expression (6). The invasive nature of biopsy might cause some complications such as bleeding, pneumothorax and thrombosis (7). So, some patients were considered not suitable for undergoing biopsy, and the heterogeneity of the tumor (necrosis or bleeding) limited the accuracy of biopsy to some extent (6,8). Some patients have lost the opportunity of undergoing surgery due to advanced tumor staging, and so tumor excision cannot be achieved.

Some previous studies have attempted to use noninvasive conventional imaging methods (such as conventional mixed-energy CT or 18F-FDG PET/CT) to evaluate Ki-67 expression *in vivo*. These studies mainly focused on the correlation of tumor and imaging findings (9-11). Compared with conventional CT, several functional parameters from different dimensions were considered by energy spectral CT, such as iodine concentration (IC), normalized iodine concentration (NIC), and distinct values at single-energy CT, were used for quantitative evaluation of tumor pathologic classification, staging and other prognostic biomarkers (TTF-1, EGFR and MVD) (12-14).

However, the prediction performance of dual-energy CT features for Ki-67 expression has been less discussed before. So, this study aimed to investigate the predictive value of energy spectral parameters for Ki-67 expression. We present the following article in accordance with the STARD reporting checklist (available at <http://dx.doi.org/10.21037/tcr-19-2769a>).

## Methods

### *Clinical data*

The study was conducted in accordance with the Declaration of Helsinki (as revised in 2013). The study is approved by the Ethics Committee of Xuzhou Medical University Hospital (ID: XYFY2018-KL097-01). This retrospective study has waived off the informed consent by our institution. Between January 2019 and May 2019, 77 patients with primary lung cancer who underwent surgical excision were included in this study (*Figure 1*). Dual-energy CT at dual-phase scanning (i.e., at the arterial and venous phases) was performed before treatment.

Inclusion criteria were as follows: patients (I) confirmed with lung cancer by surgical pathology; (II) who did not receive any relevant treatment before undergoing CT examination; (III) who did not undergo Ki-67 immunochemical analysis before; (IV) with an interval of dual-energy CT scanning and Ki-67 analysis of less than 2 weeks; and (V) with at least one measurable lesion used for imaging segmentation.

Exclusion criteria were as follows: patients (I) complicated with other malignancies and has history of any treatment; (II) with benign neoplasm or lung metastasis as confirmed by pathological examination; (III) with incomplete clinicopathological data or missed dual-energy CT examination imaging; and (IV) with the quality of images does not meet the needs of this study.

Finally, 27 cases were enrolled in this retrospective study.

### *Dual-energy CT examination protocol*

All patients underwent a dual-phase enhancement dual-energy chest scan by Siemens dual source CT scanner (SOMATOM Force, Siemens Healthcare, Forchheim, Germany). The area from the tip of the lung till the base of the lung during deep inspiration was scanned. The non-ionic iodine contrast agent (iodohydrin injection, containing 350 mg/mL iodine, GE Pharma. Shanghai co., Ltd.) was administered into the median elbow vein at a rate of 2.5 mL/s using a two-cylinder high-pressure syringe (Germany Ulrich Medical Co., Ltd., Missouri-XD2001) according to the standard of 1.0 mL/kg body weight. Next, 20 mL normal saline was used to wash at a speed of 3.0 mL/s to reduce the residual contrast agent in the vena cava and reduce the artifacts. The whole scanning time was about 70 seconds. The automatic scanning grouting tracking

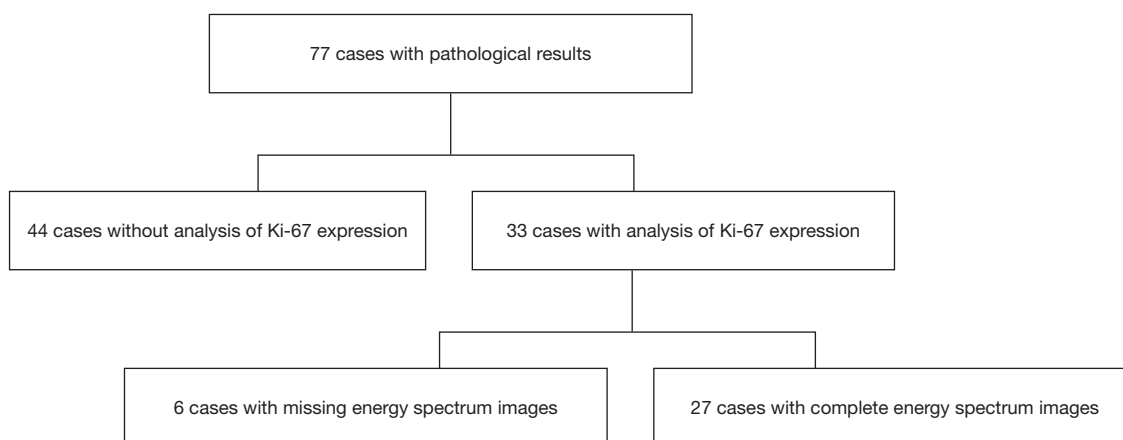


**Figure 1** Flow chart of enrolled patients in this study.

**Table 1** The other detailed dual-energy CT scanning parameters

Parameters	Values
X-ray tube rotation time (s)	0.25
Detector alignment (mm)	192×0.6
Pitch (mm)	1.0
The thick of scanning (mm)	0.5
The space of scanning (mm)	0.5
The thick of reconstruction (mm)	1.0
The space of reconstruction (mm)	0.5
Convolution kernels	Qr40
Pulmonary window position (HU)	-400
Pulmonary window width (HU)	1,500
Mediastinal window position (HU)	40
Mediastinal window width (HU)	400

technology was used. The proximal descending aorta was set as the region of interest (ROI) (Z Liu, L Xie). When the triggering threshold reached to 100 HU, the delay in automatic scanning after 6 seconds was obviously triggered. The dual-energy CT scanning parameters included were as follows: A and B spherical X-ray tube voltages were 90 and 150 kV, and the reference currents were 77 and 100 mAs, respectively. The CARE Dose 4D was switched on, which is an automatic exposure control technology used to maximize the reduction of radiation dose without affecting the image quality. The other detailed parameters were presented in *Table 1*.

**Image analysis and data acquisition**

Single-energy images at 90 and 150 kV were simultaneously transferred to dual-energy workstation (syngo. via VB10, Dual Energy, Siemens, Germany) after scanning. The dual-energy image processing and analysis were performed by two radiologists (Y Meng and L Xie) with experience in chest CT for approximately 20 and 10 years, respectively. The largest single layer of tumor was chosen for segmentation. The measured parameters (the longest and the shortest diameter) by the two radiologists were averaged for further analysis. The tumor size, T stage, N stage, necrosis and ground glass opacity (GGO) were decided by the two radiologists together. M stage was evaluated by MRI of brain, abdominal ultrasound, and/or PET-CT/MRI examinations.

The iodine-based image produced by virtual imaging technology was analyzed in the dual-energy workstation (*Figure 2*). The axial tumor, which was the largest lesion, was chosen (Y Meng) for imaging segmentation in dual-phase CT. The ROI was manually delineated with a reference to 120 kV mixed-energy image (mediastinal and lung window). ROI was delineated on single-energy station in the same way, and the CT values under different single-energies showed automatic output. The spectral data were recorded in Excel table for analysis.

For multiple foci, the largest lesion was selected for analysis. The tumor morphology parameters included the longest and the shortest diameters of the tumor, necrosis and GGO.

The longest and the shortest diameters of the tumor were measured in any of the three orthogonal planes of the

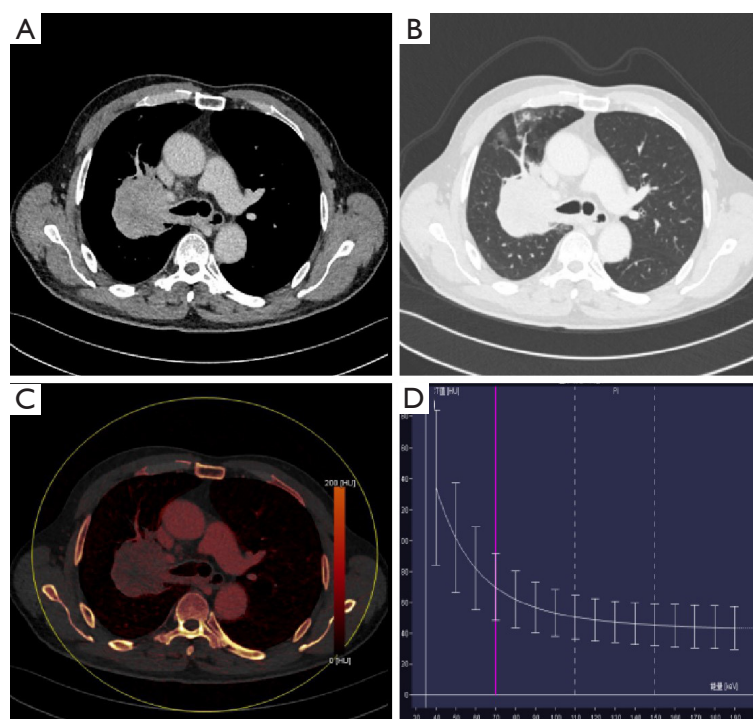


**Figure 2** A 67-year-old male with lung adenocarcinoma in the right upper lobe (Ki-67 expression, 20%). (A) mediastinal window; (B) lung window; (C) iodine graph; (D) energy spectrum curve under single-energy. The tumor was located in the hilum of the lung (A,B) with an iodine concentration (IC) of 1.2 mg/mL in venous phase (C), normalized iodine concentration (NIC) of 13.79% (C) and energy spectrum slope of 1.81 (D).

lung window (15) (*Figure S1*).

Pulmonary lesions were divided into nodules (with lesion diameter  $\leq 30$  mm) and masses (with lesion diameter  $> 30$  mm) according to the lesion size.

In the mediastinal window, necrosis was defined as low density inside the solid lesion (area large than 25%) in our study (16). GGO was defined as an increased cloudy shadow of the lung window in which the blood vessels were visible (17) (*Figure S2*).

The dual-energy parameters included IC, NIC and the slope of 40–80 keV energy spectrum curve ( $\lambda_{\text{HU}}$ ). The IC of the lesion and the aorta were measured at the same level. NIC was obtained by dividing the IC of the lesion with the IC of aorta ( $\text{NIC} = \text{IC}_{\text{lesion}}/\text{IC}_{\text{aorta}}$ ). CT values (HU) corresponding to 40 and 80 keV were measured, respectively, by calculating the slope of 40–80 keV energy spectrum curve ( $\lambda_{\text{HU}}$ ),  $\lambda_{\text{HU}} = (\text{CT}_{40 \text{ keV}} - \text{CT}_{80 \text{ keV}})/[80 - 40]$ .

Immunohistochemical analysis of the excised specimens was done by an experienced pathologist (Y Cui). All specimens were fixed with 10% formaldehyde solutions and

wrapped with wax before being cut into 4 mm serial slices. The specimens were then dewaxed with water and subjected to high-pressure antigen retrieval. A PV-9000 two-step IHC examination was performed by strictly following the manufacturer's instructions. All monoclonal antibodies of Ki-67 and kits used in this research were purchased from Beijing Zhong Shan-Golden Bridge Biological Technology Co. Ltd. (Beijing, China). The marking criteria for Ki-67 were as follows: 10 visual fields were randomly selected from each slice at high magnification, and 1,000 cells were recorded. The staining percentage of Ki-67 receptor in cell membranes and cytoplasm was calculated by using a semiquantitative method. Marking Ki-67 expression index, Ki-67 index = staining percentage of Ki-67 receptor's cell membrane and cytoplasm (*Figure S3*).

#### Statistical analysis

All data were statistically analyzed by SPSS19.0 software (SPSS Inc., Chicago, USA). The intra-group correlation

coefficient (ICC) was used to test the consistency of quantitative parameters measured by iodine-based image. The median Ki-67 expression index was used for grouping, and the enrolled patients were divided into Ki-67 high expression group and Ki-67 low expression group. Gender, age, tumor size, stage, necrosis and burr sign of the patients were considered as qualitative data, and  $\chi^2$  test was performed to compare the differences. The quantitative data such as IC,  $\lambda_{\text{HU}}$  in arterial and venous phases and NIC in the venous phase that were subjected to normal distribution were expressed as mean  $\pm$  SD, and the differences between the two groups were compared by LSD *t*-test. Rank Sum test was used to analyze the NIC in the arterial phase, which was subjected to abnormal distribution.  $P < 0.05$  was considered to be statistically significant.

## Results

### *Demographic and imaging characteristics*

Among 27 patients with lung cancer, 19 (70.4%) were male and 8 (29.6%) were female. There were 14 (51.9%) patients with age more than 60 years and 13 (48.1%)  $\leq 60$  years. The lung cancer TNM staging system was used for staging according to the 8th edition, the Union International Cancer Control (UICC) (15). Patients with T1, T2, T3 and T4 staging included 8 (29.6%), 6 (22.3%), 5 (18.5%) and 8 (29.6%), respectively. Patients with N0, N1, N2 and N3 included 9 (33.3%), 2 (7.4%), 13 (48.1%) and 3 (11.2%), respectively. Of the 27 patients, 4 (14.8%) patients had metastasis (M1) and the metastasis was located in the liver and brain, while 23 (85.2%) patients were without metastasis (M0). Four (14.8%) and 21 (77.8%) lesions were accompanied with necrosis and GGO, respectively. Nodules and masses were detected in 9 (33.3%) and 18 (66.7%) patients, respectively. Seventeen (63.0%) resected lesions were adenocarcinomatous, while 10 (37.0%) were non-adenocarcinomatous. IHC analysis revealed that 14 patients (51.9%) demonstrated high expression of Ki-67 and 13 (48.1%) patients demonstrated low expression of Ki-67 (Table 2).

### *Differences of demographic and imaging features between high and low Ki-67 expression group*

As mentioned above, 27 lung cancer patients with median Ki-67 expression index were divided into high Ki-67 expression and low expression group. The qualitative data

such as gender, age, tumor stage, the size of the lesions (long diameter, short diameter) and whether there is any necrotic lesion inside the tumor or ground-glass in appearance around the tumor were compared by using  $\chi^2$  test. Statistical analysis showed that the tumors in Ki-67 high-expression group were significantly larger than those in the low-expression group ( $P = 0.046$ ). There were no significant differences in other demographic and imaging characteristics among all enrolled patients (Table 3).

### *The ICC of dual-energy CT parameters between the two radiologists*

The correlation quantitative parameters of iodine-based images were consistent between the two observers. The mean values measured by the two observers were used for comparison and analysis between the two groups. The ICC values of IC, NIC and  $\lambda_{\text{HU}}$  were 0.983 (0.935–0.996), 0.948 (0.804–0.987) and 0.973 (0.892–0.993) (Table S1), respectively. These results proved significant consistency of dual-energy CT parameters obtained between the two radiologists.

### *The differences in dual-energy CT parameters in arterial and venous phases*

The IC, NIC and  $\lambda_{\text{HU}}$  were  $0.804 \pm 0.394$  vs.  $1.111 \pm 0.508$ ,  $0.098 \pm 0.057$  vs.  $0.303 \pm 0.137$  and  $1.623 \pm 0.889$  vs.  $2.138 \pm 1.031$  in arterial and venous phases, respectively. Compared to the energy spectral parameters in arterial phase, the IC, NIC and  $\lambda_{\text{HU}}$  values in venous phase were higher. The NIC in the venous phase was significantly higher than arterial phase ( $P < 0.01$ ), while the IC and  $\lambda_{\text{HU}}$  showed no significant differences in the two phases ( $P = 0.17$  and  $P = 0.071$ , respectively; Figure 3).

### *The differences in dual phase energy spectrum parameters between high and low Ki-67 expression group*

Figure 4 further demonstrated the distribution of energy spectral parameters in low and high Ki-67 expression subgroups. The energy spectral parameters (IC, NIC, and  $\lambda_{\text{HU}}$ ) in low Ki-67 expression were higher than those in the high Ki-67 expression subgroup. The venous phase NIC and  $\lambda_{\text{HU}}$  ( $0.249 \pm 0.083$ ,  $0.360 \pm 0.162$ ,  $P = 0.033$  in NIC and  $1.744 \pm 0.607$ ,  $2.562 \pm 1.236$ ,  $P = 0.037$  in  $\lambda_{\text{HU}}$ , respectively) showed significant differences in the two groups (Table 4,

**Table 2** Demographic characteristics of enrollment patients (n=27)

Characteristics	Number	Frequency (%)
Gender		
Male	19	70.4
Female	8	29.6
Age (median, years)		
≤60	14	51.9
>60	13	48.1
T staging (AJCC 8th)		
T1	8	29.6
T2	6	22.3
T3	5	18.5
T4	8	29.6
N staging (AJCC 8th)		
N0	9	33.3
N1	2	7.4
N2	13	48.1
N3	3	11.2
M staging (AJCC 8th)		
M0	23	85.2
M+	4	14.8
Ki-67 expression (median, %)		
Low (≤30)	13	48.1
High (>30)	14	51.9
Size (cm)		
Nodule (≤3)	9	33.3
Mass (>3)	18	66.7
Longest diameter (median, mm)		
≤42.8	14	51.9
>42.8	13	48.1
Shortest diameter (median, mm)		
≤33.6	14	51.9
>33.6	13	48.1
Ground-glass opacity (GGO)		
Yes	21	77.8
No	6	22.2
Necrosis		
Yes	4	14.8
No	23	85.2
Histological type		
Adenocarcinoma	17	63.0
Squamous-cell carcinoma	7	25.9
Small cell lung cancer	3	11.1

T staging, primary tumor staging; N staging, regional lymph node staging; M staging, distant metastasis staging; Ki-67, a protein that is encoded by MKI-67 gene in humans.

Figure 4). The differences in other energy spectral parameters in arterial and venous phases were also analyzed, but showed no significant differences in the arterial phase IC, NIC,  $\lambda_{HU}$  and venous phase IC between high and low Ki-67 expression groups (P values ranged from 0.105 to 0.182). Furthermore, venous phase energy spectral parameters (IC, NIC,  $\lambda_{HU}$ ) were higher than arterial phase in low and high Ki-67 expression subgroups (P=0.054–0.259), but the differences showed no significance.

### The performance of energy spectral parameters for predicting Ki-67 expression

To further explore the predictive efficacy of NIC and  $\lambda_{HU}$  on Ki-67 expression, the ROC curve of the venous phase NIC and  $\lambda_{HU}$  was plotted. The ROC analysis of venous phase NIC (vpNIC) showed borderline P value (P=0.056) with AUC (P=0.056). The sensitivity (SE), specificity (SP) and cut-off value were 0.717, 92.86, 61.54 and ≤0.347 for vpNIC, respectively. The AUC, SE, SP, and cut-off value of SP were 0.698, 92.86, 53.85 and ≤2.407, respectively (Table 5, Figure 5).

### Discussion

In this study, vpNIC and vp $\lambda_{HU}$  were significantly different in high and low Ki-67 expression groups (P=0.033 and 0.037, respectively). The performance of vpNIC and vp $\lambda_{HU}$  for predicting Ki-67 expression were 0.717 and 0.698, respectively. The dual-energy spectral parameters (IC, NIC and  $\lambda_{HU}$ ) of venous phase were higher than the arterial phase. Furthermore, the low expression Ki-67 group was associated with higher IC, NIC and  $\lambda_{HU}$  values when compared to high expression group.

The high expression group had relatively larger tumor volume in this study. Ki-67 high expression reflected more tumor aggressiveness, faster growth, and lower microvessel density (18). Previous studies demonstrated that greater proliferation of tumor is accompanied with relatively worse blood supply in the central portion (19,20). The aggressiveness of lung cancer with poorer differentiation showed more necrosis (21). In our study, higher NIC and  $\lambda_{HU}$  in the venous phase were associated with less aggressive lesions (low Ki-67 expression group). Our results were not completely in line with the study conducted by Spira *et al.* (21), as necrosis showed no significant differences in low and

**Table 3** Differentiation of low and high expression groups of Ki-67 (n=27)

Characteristics	Low Ki-67, n (%)	High Ki-67, n (%)	P
Gender			0.678
Male	10 (37.037)	9 (33.333)	
Female	3 (11.111)	5 (18.519)	
Age (median, years)			1.000
≤60	7 (25.926)	7 (25.926)	
>60	6 (22.222)	7 (25.926)	
T staging (AJCC 8th)			0.706
T1-2	6 (22.222)	8 (29.630)	
T3-4	7 (25.926)	6 (22.222)	
N staging (AJCC 8th)			0.236
Negativity	6 (22.222)	3 (11.111)	
Positivity	7 (25.926)	11 (40.741)	
M staging (AJCC 8th)			0.326
Negativity	10 (37.037)	13 (48.148)	
Positivity	3 (11.111)	1 (3.704)	
Nodule (diameter ≤3 cm)			0.046*
Yes	7 (25.926)	2 (7.407)	
No	6 (22.222)	12 (44.444)	
Longest diameter (median, mm)			0.280
≤42.8	8 (29.630)	6 (22.222)	
>42.8	5 (18.519)	8 (29.630)	
Shortest diameter (median, mm)			0.280
≤33.6	8 (29.630)	6 (22.222)	
>33.6	5 (18.519)	8 (29.630)	
Ground-glass shadow			0.648
Yes	10 (37.037)	12 (44.444)	
No	3 (11.111)	2 (7.407)	
Necrosis			1.000
Yes	2 (7.407)	2 (7.407)	
No	11 (40.741)	11 (40.741)	

\*, significant difference between low and high Ki-67 groups. T staging, primary tumor staging; N staging, regional lymph node staging; M staging, distant metastasis staging; Ki-67, a protein that is encoded by MKI-67 gene in humans.

high expression group (P=1.000). Several study results showed that NIC and  $\lambda_{HU}$  parameters might effectively reflect the different chemical composition characteristics of tumors (22-24). So, we speculated that energy spectral

parameters (NIC and  $\lambda_{HU}$ ) were superior to traditional morphologic features in order to evaluate the tumor microstructure change caused by microvessel density and hypovascular in more aggressive lung cancer early. This

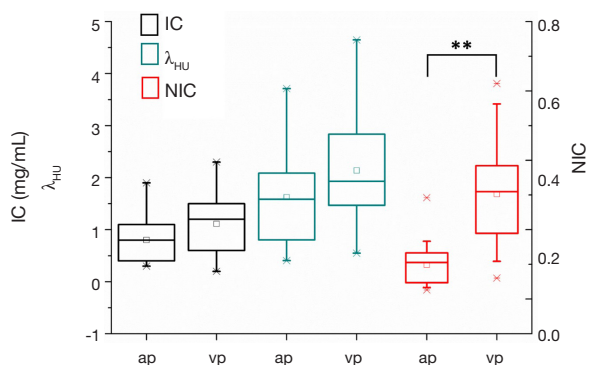


**Figure 3** The box plots of the arterial and venous phases energy spectrum CT parameters. \*\* $P < 0.01$ .

**Table 4** The differences of arterial and venous phase energy spectrum CT parameters in low and high Ki-67 groups (mean  $\pm$  SD)

Variables	Low Ki-67	High Ki-67	P
AP			
IC	0.923 $\pm$ 0.453	0.693 $\pm$ 0.308	0.132
NIC	0.115 $\pm$ 0.019	0.083 $\pm$ 0.011	0.105
$\lambda_{\text{HU}}$	1.863 $\pm$ 1.077	1.400 $\pm$ 0.631	0.182
VP			
IC	1.262 $\pm$ 0.581	0.971 $\pm$ 0.401	0.141
NIC	0.360 $\pm$ 0.162	0.249 $\pm$ 0.083	0.033*
$\lambda_{\text{HU}}$	2.562 $\pm$ 1.236	1.744 $\pm$ 0.607	0.037*

\*, significant differences in low and high Ki-67 index ( $P < 0.05$ ). IC, iodine concentration; NIC, normalized iodine concentration;  $\lambda_{\text{HU}}$ , the slope of the 40–80 keV energy spectrum curve; AP, arterial phase; VP, venous phase.

result was consistent with the study conducted by Lin and colleagues on non-small cell lung cancer (NSCLC) (25). However, due to smaller sample size in our study, the results require further validation in next study.

In the whole cohort and subgroup analysis, the venous phase energy spectral parameters were all higher than those of arterial phase. Yang and colleagues on NSCLC lymph node involvement research also showed that the venous phase parameters were higher than the arterial phase parameters (26). In venous phase, the concentration of iodine contrast agent reached peak. Also a previous study demonstrated that iodine-based image was superior to that of mixed-energy image for monitoring the change of IC (27).

So, the dual energy perfusion imaging might offer more detailed perfusion information to calculate the changes of these parameters in different phases.

There were no significant differences for IC and other arterial phase parameters. The reason for this might be due to that IC itself was influenced by various factors, such as the total dose of contrast medium, flow rate of injection, and individual differences in circulation (28), while standardization of IC (reference aorta of the same layer) might effectively eliminate these biases. Furthermore, the difference in concentration between tumor and aorta might also exist to a certain extent, explaining that vpNIC and vp $\lambda_{\text{HU}}$  in the two groups showed significant differences.

The model constructed by energy spectral parameters (vpNIC and vp $\lambda_{\text{HU}}$ , respectively) showed effective performance for predicting Ki-67 expression (AUC = 0.717 and 0.698, respectively). Some researches revealed that breast cancer Ki-67 expression level showed significant association with tumor pathologic complete response (pCR) and prognosis after undergoing neoadjuvant chemotherapy (29–31). In contrast to other invasive methods, the dual energy CT parameters demonstrated high noninvasive stratification and low risk Ki-67 expression before treatment. So, monitoring tumor biomarker (Ki-67) offered more baseline individualized information to improve treatment response and outcomes in lung cancer patients. Compared to sensitivity, inferior specificity results were shown in this study. So, combining other biomarkers is warranted to further improve the model performance.

In this study, we analyzed the application value of energy spectrum parameters in lung cancer Ki-67 expression. The energy spectral parameters of venous phase might be used for predicting Ki-67 stratification. The highlight of this study was noninvasive to predict Ki-67 expression level. For other neoplasm, pre-surgery immunochemistry stratification for patients may offer more valuable treatment information. Furthermore, some patients did not perform biopsy or surgical treatment for different reasons, this noninvasive CT imaging method may help oncologists to development an optimal regimen. Therefore, the clinical value of energy spectrum CT in other different tumors need to further discussion. In the study, we did not discuss the healthy controls results. The following were reasons: (I) the region of interest (ROI) was difficult to delineate for lack of specific lesions; (II) because the healthy controls did not perform surgery or biopsy, the results of pathology were

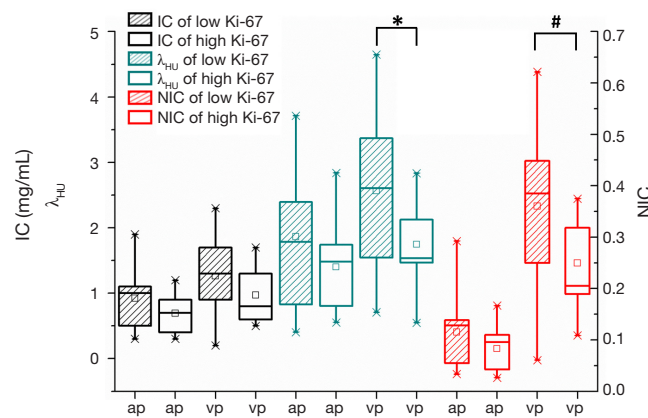


**Figure 4** The box plots of the arterial and venous phase energy spectrum CT parameters between low and high Ki-67 groups. Venous phase  $\lambda_{HU}$  and NIC showed significant differences between low and high Ki-67 expression groups ( $P<0.05$ ). \*, the venous phase  $\lambda_{HU}$  of low Ki-67 group in comparison with high Ki-67 group,  $P<0.05$ . #, the venous phase NIC of low Ki-67 group in comparison with high Ki-67 group,  $P<0.05$ .

**Table 5** ROC curve analysis of energy spectrum CT parameters

Variables	AUC (95% CI)	SE	SP	Cut-off value	P
vpNIC	0.717 (0.512–0.872)	92.86	61.54	$\leq 0.347$	0.056
vp $\lambda_{HU}$	0.698 (0.492–0.858)	92.86	53.85	$\leq 2.407$	0.077

vpNIC, normalized iodine concentration of venous phase; vp $\lambda_{HU}$ , slope of the 40–80 keV energy spectrum curve of venous phase.

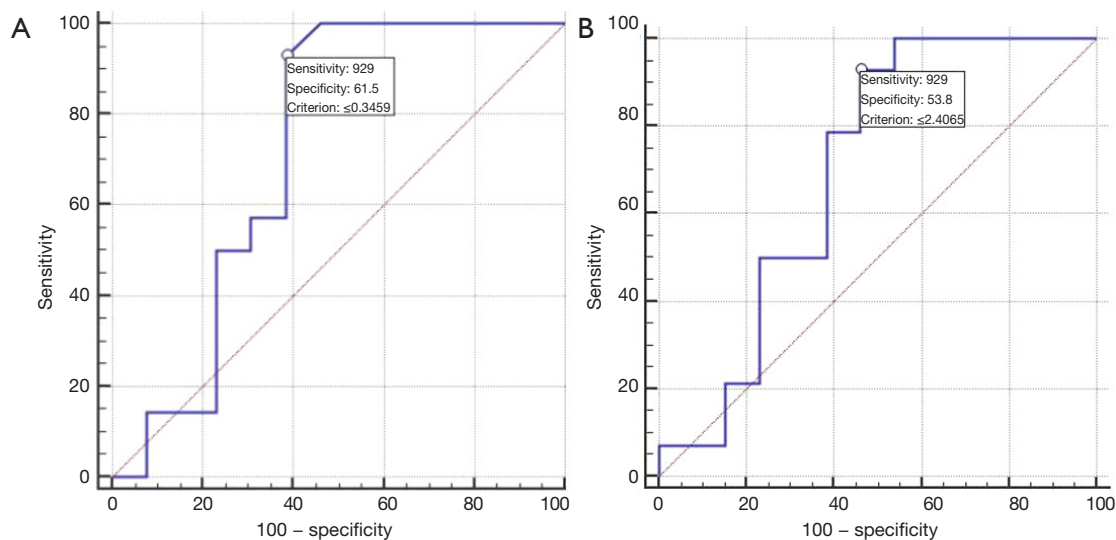


**Figure 5** The ROC curve of vpNIC (A) and vp $\lambda_{HU}$  (B). (A) the AUC, SN, SP and cutoff values of vpNIC were 0.717, 92.86, 61.54 and 0.347, respectively ( $P=0.056$ ). (B) the AUC, SN, SP and cutoff value of vp $\lambda_{HU}$  were 0.698, 92.86, 53.85 and 2.407, respectively ( $P=0.077$ ).

not accessed in clinical work.

However, there were some limitations in this study. Firstly, a relatively small sample size cannot completely reflect the relation of dual energy features and Ki-67 expression. Secondly, the predictive value of energy spectral parameters of other lung cancer prognostic biomarkers (TTF-1, EGFR and Grade of tumor differentiation) was not investigated. The whole volume tumor segmentation was not used in this study. The whole volume tumor segmentation required vast time, and so was not completely suitable in clinical practice. Previous study results showed that the whole tumor segmentation methodology with relatively inferior consistency was related to the largest single section method (32). Finally, the real outcomes of high and low Ki-67 expression groups in patients were not explored due to lack of enough survival time.

So, the energy spectral parameters of venous phase might be used for predicting Ki-67 stratification. The energy spectral parameters of venous phase were higher than the arterial phase. Furthermore, the low expression Ki-67 group had higher IC, NIC and  $\lambda_{HU}$  than high expression group.

### Acknowledgments

**Funding:** We acknowledge financial support from National Natural Science Foundation of China (81771904), Jiangsu Commission of Health (Z2018037), Xuzhou Science and Technology Program (KC15SX004), NYMU & Far Eastern Memorial Hospital (107DN13), NYMU & Cheng-Hsin General Hospital (CY10823).

### Footnote

**Reporting Checklist:** The authors have completed the STARD reporting checklist. Available at <http://dx.doi.org/10.21037/tcr-19-2769a>

**Data Sharing Statement:** Available at <http://dx.doi.org/10.21037/tcr-19-2769a>

**Conflicts of Interest:** All authors have completed the ICMJE uniform disclosure form (available at <http://dx.doi.org/10.21037/tcr-19-2769a>). The authors have no conflicts of interest to declare.

**Ethical Statement:** The authors are accountable for all aspects of the work in ensuring that questions related

to the accuracy or integrity of any part of the work are appropriately investigated and resolved. The study was conducted in accordance with the Declaration of Helsinki (as revised in 2013). The study is approved by the Ethics Committee of Xuzhou Medical University Hospital (ID: XYFY2018-KL097-01). This retrospective study has waived off the informed consent by our institution.

**Open Access Statement:** This is an Open Access article distributed in accordance with the Creative Commons Attribution-NonCommercial-NoDerivs 4.0 International License (CC BY-NC-ND 4.0), which permits the non-commercial replication and distribution of the article with the strict proviso that no changes or edits are made and the original work is properly cited (including links to both the formal publication through the relevant DOI and the license). See: <https://creativecommons.org/licenses/by-nc-nd/4.0/>.

### References

1. Kang J, Galluzzi L. PD-L1 blockade for urothelial carcinoma. *Oncoimmunology* 2017;6:e1334028.
2. Li J, Guo W, Ran J, et al. Five-year lung cancer mortality risk analysis and topography in Xuan Wei: a spatiotemporal correlation analysis. *BMC Public Health* 2019;19:173.
3. Ross DT, Scherf U, Eisen MB, et al. Systematic variation in gene expression patterns in human cancer cell lines. *Nat Genet* 2000;24:227-35.
4. Martin B, Paesmans M, Mascaux C, et al. Ki-67 expression and patients survival in lung cancer: systematic review of the literature with meta-analysis. *Br J Cancer* 2004;91:2018-25.
5. Ishibashi N, Maebayashi T, Aizawa T, et al. Correlation between the Ki-67 proliferation index and response to radiation therapy in small cell lung cancer. *Radiat Oncol* 2017;12:16.
6. Li Y, Pan Y, Wang R, et al. ALK-rearranged lung cancer in Chinese: a comprehensive assessment of clinicopathology, IHC, FISH and RT-PCR. *PLoS One* 2013;8:e69016.
7. Tomiyama N, Yasuhara Y, Nakajima Y, et al. CT-guided needle biopsy of lung lesions: a survey of severe complication based on 9783 biopsies in Japan. *Eur J Radiol* 2006;59:60-4.
8. Shan L, Lian F, Guo L, et al. Detection of ROS1 Gene Rearrangement in Lung Adenocarcinoma: Comparison of IHC, FISH and Real-Time RT-PCR. *PLoS One* 2015;10:e0120422.

9. Sauter AW, Winterstein S, Spira D, et al. Multifunctional Profiling of Non-Small Cell Lung Cancer Using 18F-FDG PET/CT and Volume Perfusion CT. *J Nucl Med* 2012;53:521-9.
10. Wang JY, Dong D, Dai CL, et al. Correlation of CT presentation with histo-differentiation and p53 and Ki-67 expressions in gastric cancer. *Zhongguo Yi Xue Ke Xue Yuan Xue Bao. Acta Academiae Medicinae Sinicae* 2011;33:555-9.
11. Abgral R, Leboulleux S, Déandris D, et al. Performance of 18Fluorodeoxyglucose-Positron Emission Tomography and Somatostatin Receptor Scintigraphy for High Ki-67 ( $\geq 10\%$ ) Well-Differentiated Endocrine Carcinoma Staging. *J Clin Endocrinol Metab* 2011;96:665-71.
12. Thieme SF, Graute V, Nikolaou K, et al. Dual Energy CT lung perfusion imaging--correlation with SPECT/CT. *Eur J Radiol* 2012;81:360-5.
13. McCollough CH, Leng S, Yu L, et al. Dual- and Multi-Energy CT: Principles, Technical Approaches, and Clinical Applications. *Radiology* 2015;276:637-53.
14. Li GJ, Gao J, Wang GL, et al. Correlation between vascular endothelial growth factor and quantitative dual-energy spectral CT in non-small-cell lung cancer. *Clin Radiol* 2016;71:363-8.
15. Goldstraw P, Chansky K, Crowley J, et al. The IASLC Lung Cancer Staging Project: Proposals for? Revision of the TNM Stage Groupings in the Forthcoming (Eighth) Edition of the TNM Classification for Lung Cancer. *J Thorac Oncol* 2016;11:39-51.
16. Jiang M, Lu HY, Shan XH, et al. CT quantitative analysis study for angiogenesis, and degree of ischemic necrosis and glucose metabolite in non-small cell lung cancer. *Eur Rev Med Pharmacol Sci* 2018;22:4146-55.
17. Kim HY, Shim YM, Lee KS, et al. Persistent Pulmonary Nodular Ground-Glass Opacity at Thin-Section CT: Histopathologic Comparisons. *Radiology* 2007;245:267-75.
18. Krüger K, Stefansson IM, Collett K, et al. Microvessel proliferation by co-expression of endothelial nestin and Ki-67 is associated with a basal-like phenotype and aggressive features in breast cancer. *Breast* 2013;22:282-8.
19. Zhu YH, Wang X, Zhang J, et al. Low enhancement on multiphase contrast-enhanced CT images: an independent predictor of the presence of high tumour grade of clear cell renal cell carcinoma. *AJR Am J Roentgenol* 2014;203:W295-300.
20. Miles KA. Tumour angiogenesis and its relation to contrast enhancement on computed tomography: a review. *Eur J Radiol* 1999;30:198-205.
21. Spira D, Neumeister H, Spira SM, et al. Assessment of tumour vascularity in lung cancer using volume perfusion CT (VPCT) with histopathologic comparison: a further step toward an individualized tumour characterization. *J Comput Assist Tomogr* 2013;37:15-21.
22. Karçaaltuncaba M, Aktas A. Dual-energy CT revisited with multidetector CT: review of principles and clinical applications. *Diagn Interv Radiol* 2011;17:181-94.
23. De Cecco CN, Darnell A, Rengo M, et al. Dual-energy CT: oncologic applications. *AJR Am J Roentgenol* 2012;199:S98-105.
24. Fornaro J, Leschka S, Hibbeln D, et al. Dual-and multi-energy CT: approach to functional imaging. *Insights Imaging* 2011;2:149-59.
25. Lin LY, Zhang Y, Suo ST, et al. Correlation between dual-energy spectral CT imaging parameters and pathological grades of non-small cell lung cancer. *Clin Radiol* 2018;73:412.e1-7.
26. Yang F, Dong J, Wang X, et al. Non-small cell lung cancer: Spectral computed tomography quantitative parameters for preoperative diagnosis of metastatic lymph nodes. *Eur J Radiol* 2017;89:129-35.
27. Gordic S, Puipe GD, Krauss B, et al. Correlation between Dual-Energy and Perfusion CT in Patients with Hepatocellular Carcinoma. *Radiology* 2016;280:78-87.
28. Lin JZ, Zhang L, Zhang CY, et al. Application of gemstone spectral computed tomography imaging in the characterization of solitary pulmonary nodules: preliminary result. *J Comput Assist Tomogr* 2016;40:907-11.
29. Denkert C, Loibl S, Muller BM, et al. Ki-67 levels as predictive and prognostic parameters in pretherapeutic breast cancer core biopsies: a translational investigation in the neoadjuvant GeparTrio trial. *Ann Oncol* 2013;24:2786-93.
30. Miura D, Hasegawa Y, Horiguchi J, et al. Abstract PD3-7: Disease-free survival and Ki-67 analysis of a randomized controlled trial comparing zoledronic acid plus chemotherapy with chemotherapy alone as a neoadjuvant treatment in patients with HER2-negative primary breast cancer (JONIE-1 study). *Cancer Res* 2013;73.
31. Schlotter CM, Tietze L, Vogt U, et al. Ki-67 and lymphocytes in the pretherapeutic core biopsy of primary

- invasive breast cancer: positive markers of therapy response prediction and superior survival. *Horm Mol Biol Clin Investig* 2017. doi: 10.1515/hmbci-2017-0022.
32. Ng QS, Goh V, Fichte H, et al. Lung Cancer Perfusion

at Multi-Detector Row CT: Reproducibility of Whole Tumor Quantitative Measurements. *Radiology* 2006;239:547-53.

**Cite this article as:** Dou P, Liu Z, Xie L, Meng C, Wang C, Cui Y, Hu C, Cheng G, Chen J, Meng Y, Xu K. The predictive value of energy spectral CT parameters for assessing Ki-67 expression of lung cancer. *Transl Cancer Res* 2020;9(7):4267-4278. doi: 10.21037/tcr-19-2769a

**Table S1** ICC of energy spectrum CT parameters between two radiologists

Variables	ICC	95% CI
IC	0.983	0.935–0.996
NIC	0.948	0.804–0.987
$\lambda_{\text{HU}}$	0.973	0.892–0.993

IC, iodine concentration; NIC, normalized iodine concentration;  $\lambda_{\text{HU}}$ , the slope of 40–80 keV energy spectrum curve; ICC, Intra-class correlation coefficient.

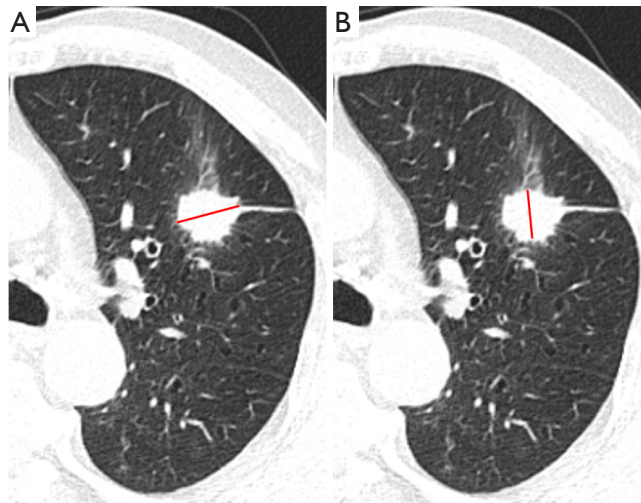


**Figure S1** A 67-year-old male with lung carcinoma in the left upper lobe of the lung. (A,B) The measurement of the shortest and the longest diameters by a radiologist. (A) The shortest diameter of the lesion was 1.9 mm; (B) The longest diameter of the lesion was 2.4 mm.

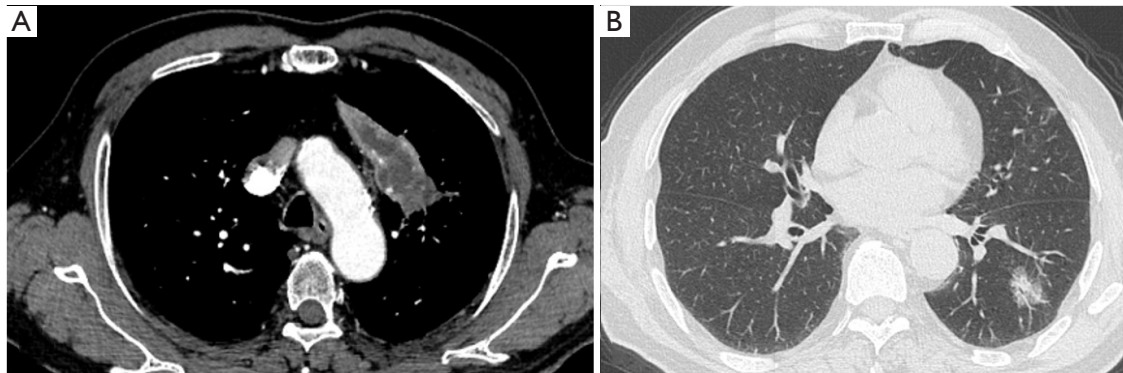


**Figure S2** CT findings of necrosis and ground glass opacity (GGO). (A) A 48-year-old male with lung carcinoma in the left upper lobe of the lung. The necrosis showed delineation in the lesion and the necrosis area was larger than 25%. (B) A 76-year-old female with lung carcinoma in the left lower lobe of the lung. The lung window showed mixed GGO.

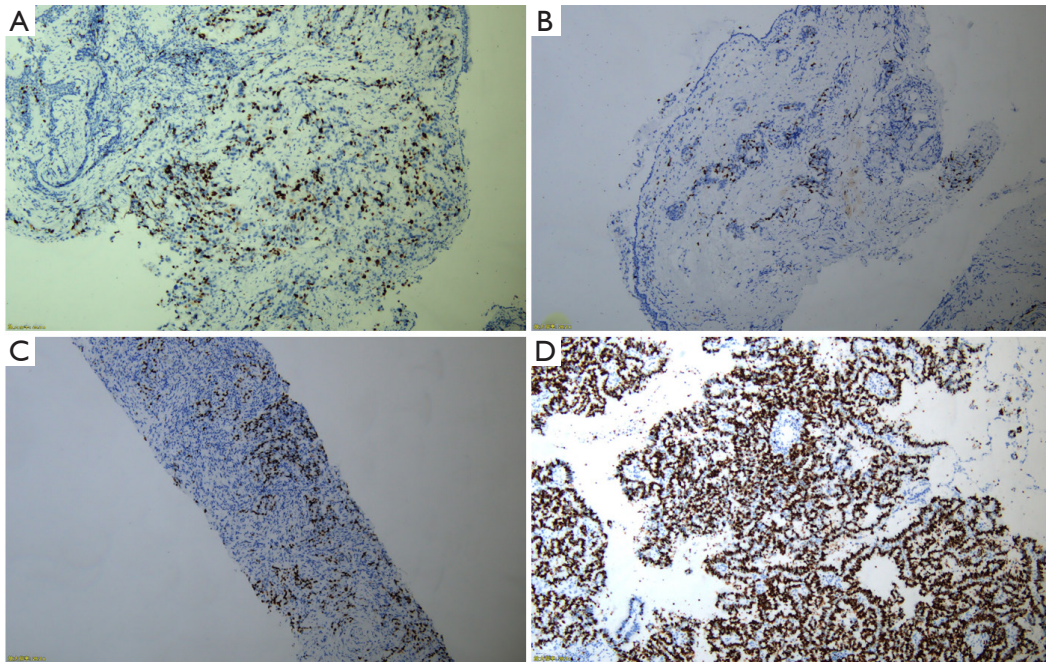


**Figure S3** Immunohistochemical staining of 4 cases ( $\times 100$ ). (A,B) Ki-67 low expression (20%); (C,D) high expression of Ki-67 (C: 60%; D: 80%).